Environmental Science and Pollution Research (2022) 29:29478–29497
https://doi.org/10.1007/s11356-021-15880-5

THE INTERACTION BETWEEN ENVIRONMENTAL POLLUTION AND CULTURAL HERITAGE: FROM OUTDOOR TO INDOOR

Multitechnique diagnostic analysis and 3D surveying prior to the restoration of *St. Michael defeating Evil* painting by Mattia Preti

Sebastiano D'Amico[1] · Valeria Comite[2] · Giuseppe Paladini[3] · Michela Ricca[4] · Emanuele Colica[1] · Luciano Galone[1] · Sante Guido[5] · Giuseppe Mantella[6] · Vincenza Crupi[7] · Domenico Majolino[3] · Paola Fermo[2] · Mauro Francesco La Russa[4] · Luciana Randazzo[4] · Valentina Venuti[3]

Received: 7 April 2021 / Accepted: 5 August 2021 / Published online: 13 August 2021

Abstract

In this study, a multimethodological analysis involving optical and physical/chemical diagnostic techniques and 3D photogrammetric survey was successfully applied, for the first time, on the large oil on canvas *St. Michael defeating Evil* painting by Mattia Preti, located inside the Church of the Immaculate Conception of Sarria (Floriana) in Malta. Pigmenting agents, binder media, and raw materials were first characterized, both at elemental and molecular scales, through X-ray fluorescence spectroscopy (XRF), optical stereo microscopy (SM), scanning electron microscopy coupled with energy dispersive X-ray spectroscopy (SEM-EDX), Fourier transform infrared spectroscopy (FT-IR), and gas chromatography coupled with mass spectrometry (GC-MS). The main goal was to properly identify the execution technique of this famous painter, the artist's palette, and possible nondocumented interventions. The 3D photogrammetric survey, on the other side, allowed us to noninvasively evaluate the extension of the areas that experienced restorations, and to properly map the domains of the different canvasses observed. The joints between canvasses suggested that the painting was folded and rolled up. In addition, the employment of a thermal camera gave evidence of the different consolidating material injection points used during the restoration to strengthen the painting. The obtained results offer useful information for the development of optimized restoration and conservation strategies to be applied and provide, at the same time, answers to open questions related to provenance and dating of the investigated artwork.

Keywords Conservation · Lunette · Mattia Preti · Pigment's identification · Globigerina limestone · Multitechnique analysis · 3D photogrammetric survey

Sebastiano D'Amico and Valeria Comite contributed equally to this work.

Responsible Editor: Michel Sablier

✉ Giuseppe Paladini
gpaladini@unime.it

✉ Michela Ricca
michela.ricca@unical.it

[1] Department of Geosciences, University of Malta, Msida Campus, Msida MSD2080, Malta

[2] Department of Chemistry, University of Milan, Via Golgi 19, 20133 Milan, Italy

[3] Department of Mathematical and Computer Sciences, Physical Sciences and Earth Sciences, University of Messina, Viale Ferdinando Stagno D'Alcontres 31, I-98166 Messina, Italy

[4] Department of Biology, Ecology and Earth Sciences, University of Calabria, 87036 Arcavacata di Rende (CS), Italy

[5] Department of Literature and Philosophy, University of Trento, Via Tommaso Gar 14, I-38122 Trento, Italy

[6] Giuseppe Mantella Restauro Opere D'Arte, Circonvallazione Paparo 25, 88060 Isca sullo Ionio (CZ), Italy

[7] Department of Chemical, Biological, Pharmaceutical and Environmental Sciences, University of Messina, Viale Ferdinando Stagno D'Alcontres 31, I-98166 Messina, Italy

Introduction

The *St. Michael defeating Evil* painting is a masterpiece of the painter Mattia Preti, a renowned Italian artist active in Malta between 1661 and 1699, year of his death. It is one of the seven paintings that Mattia Preti executed inside the Church of the Immaculate Conception of Sarria (Fig. 1a-c) in Floriana (Malta), in occasion of its reconstruction in 1677 as *ex voto* for the end of the plague in 1676. The Church, commissioned by the Grand Master of the Knights of Malta, friar Nicolas Cottoner, is characterized by a central plan almost totally designed by Mattia Preti himself. The pictorial cycle includes five paintings depicting *Mary Immaculate and the Saints protectors from the plague* and, painted on two large Lunettes, two examples of the *struggle of Good against Evil* in relation to the plague disease interpreted as divine punishment. These "oil on canvas" paintings were all executed between 1677 and 1679, and are essentially inspired to subjects that Mattia Preti had depicted almost twenty years earlier in seven frescoes, on many gates of the city of Naples, as *ex voto* for the end of the plague epidemic in 1656.

The *St. Michael defeating Evil* painting, under investigation in the present study, is one of the two Lunettes of the arches (see Fig. 1d), together with the *Allegory of the Order of St. John the Baptist* painting (Fig. 1e). This large-sized (235 cm × 475 cm) work depicts the exterminating Archangel dressed as a Knight of the Order of Malta, with armor and bright red cloak, as he bursts from above holding his sword at the head of a host of executioner angels armed with foils and lightning bolts, ready to punish demons, offenders and sinners depicted in a tangle of lifeless bodies or dismayed and subjugated by terror.

At the beginning of the restoration process, the painting appeared seriously damaged, being the canvas compromised and the pictorial surface severely repainted and darkened by oils and waxes applied over the years. Therefore, it was necessary to study the dramatic state of conservation of the painting thanks to archival research, in order to understand the problems of the work and to plan the most appropriate scientific investigations to be executed.

In particular, it was understood that over the centuries the Lunette had undergone several conservation interventions, two of which documented by archival sources.

In the 30s of the twentieth century, considering the poor conservation conditions (the painting must have already been very incomplete) it was reupholstered on a new canvas.

The work was the subject of a very bad lining operation which involved the almost complete detachment of the original canvas and the application on a new canvas only of the preparation and the pictorial film. The gluing was performed with animal glue, not very elastic, which in few years, due to a polymerization process, stiffened the painting to completion. During this operation, the numerous gaps created were filled with plaster and glue colored with iron oxide, in order to match them chromatically with the original brown-colored preparation by Mattia Preti. By means of oil colors, the gaps

Fig. 1 **a** Map of Malta, with the town of Floriana indicated. **b** External and **c** internal view of the Church of the Immaculate Conception of Sarria in Floriana, Malta. **d** *St. Michael defeating Evil* and **e** the *Allegory of the Order of St. John the Baptist* paintings

created with the detachment of large portions were completely repainted, and many of the original figures were reproposed.

Concerning the second documented intervention, it took place after the Second World War. At that time, the most important paintings in churches throughout the island of Malta were protected after the outbreak of the conflict by collecting and hiding them in bunkers in uninhabited areas. In particular, in the case of the *St. Michael defeating Evil* painting, the artwork was removed from the frame and rolled up. The latter operation caused very serious damages, due to the stiffening of the glue employed in the 30s, which caused the tearing of the artwork into overlapping bands. In the 50s, a new conservative intervention was carried out, during which, since the re-sheathed canvas could not be removed, a new canvas was applied over the previous one, this time with paste, unfortunately free of bactericide. In addition, new gaps were plastered and some new repaintings were carried out.

In the framework of restoration interventions, the possibility to create digital models and 3D replicates of objects/artworks of historical and artistic value has gained, in recent years, considerable attention (Yilmaz et al. 2007; Arias et al. 2007; Armesto et al. 2008; Remondino et al. 2009; Remondino 2011; Fiorillo et al. 2015; Balletti et al. 2016; Aicardi et al. 2018; D'Amico et al. 2020). It is worth of note that if, on one side, close-range photogrammetry and triangulation laser scanner permit the development of digital archives of small objects and/or small volumes, on the other side, image-based techniques allow the definition of digital archives which can be used to plan and support the different restoration phases. In addition, 3D reconstructions are quite simple to be accomplished, providing at the same time reliable information about the spatial/geometrical properties of objects and environments, basically without any direct contact. To further support the definition of optimized restoration and conservation strategies to be applied to artifacts, the multitechnique characterization, through complementary non- or, at least, micro-destructive methodologies, of the constituent materials such as pigmenting agents, binding media, and preparatory materials, represents an extremely valuable source of information (Wolbers 2000; Edwards et al. 2004; Castro et al. 2008; Bersani et al. 2008, 2014; Rosi et al. 2009; Tschegg et al. 2009; Ruffolo et al. 2010; Vizárová et al. 2011; Barbera et al. 2012; La Russa et al. 2014; Comite and Ricca 2016; Crupi et al. 2018; Ricca et al. 2019; Chelazzi et al. 2020; Fermo et al. 2020; Venuti et al. 2020; Zuena et al. 2020) in order to give answers concerning open problems such as execution technique, dating, and provenance.

With particular regard to previous studies on Mattia Preti painting materials and technique, G. Chiavari et al. (Chiavari et al. 2007) conducted, in 2007, a diagnostic survey on the *Dinner of Emmaus* painting (oil on canvas) by Mattia and Gregorio Preti (private collection), through the employment of several morphological and chemical tecniques including optical stereo microscopy (SM), scanning electron microscopy coupled with energy dispersive X-ray spectroscopy (SEM-EDX), and gas chromatography coupled with mass spectrometry (GC-MS). The investigation was aimed at characterizing binders, pigments, and stratigraphy of the samples in order to understand the painting technique, achieving information that could support the hypothesis, formulated by stylistic considerations, of the presence of Mattia in Gregorio's work. Later in 2018, C. Pelosi et al. (Pelosi et al. 2018) carried out a multimethodological scientific investigation involving infrared reflectometry, X-ray radiography, polarized light microscopy, Fourier transform infrared spectroscopy (FT-IR), and Raman tecniques on three different paintings by Mattia Preti, namely *The penitent St. Peter* (oil on canvas)*, St. Peter blessing* (oil on canvas), and the *Madonna of Sorrows* (oil on canvas), owned by the Wignacourt College Museum of Rabat, in Malta, focusing their attention on the late production activity of the artist. The composition, with particular regard to the stratigraphy of the paintings, was clarified, supporting the restoration works in progress at that time. During the same period, a noninvasive diagnostic campaign, by means of X-ray radiography and X-ray fluorescence spectroscopy (XRF), was carried out on the *Allegory of the five senses* (oil on canvas) by Mattia and Gregorio Preti (Barberini Corsini collection), providing evidences of the execution tecnique employed by the painters, as well as the elemental composition of the pigmenting agents used (Ridolfi 2019). Recently, our research group assessed a detailed scientific examination on the newly-restored painting entitled *The Conversion of St. Paul* (oil on canvas) by Mattia Preti, placed above the main altar of the Cathedral of Mdina, in Malta (D'Amico et al. 2021). In particular, the employment of a combined approach involving digital 3D photogrammetric survey, XRF and Raman techniques allowed us to successfully develop a 3D model of the investigated work of art and, at the same time, permitted the identification/characterization of the artist's palette. The potentialities of the combined use of 2D/3D photogrammetric surveys, in order to achieve reconstruction, and XRF and Raman spectroscopies, for the pigments identification, were successfully exploited prior to, during and after the recent restoration of the painting.

In this work, a preliminary *in situ* investigation, through portable XRF, of the *St. Michael defeating Evil* painting allowed the identification, at the elemental scale, of the composition of some representative areas, in terms of major and minor constituents. Then, a sampling procedure was performed in order to assess the samples stratigraphy, and to better understand the pigment's palette and the raw materials used by the artist for the preparatory layer and for the painting, by applying SM and SEM-EDX. In addition, FT-IR spectroscopy was adopted to primarily identify mineralogical phases although the technique, in the field of Cultural Heritage, is mainly used for the identification of the organic ones. In the

specific case, investigations were carried out to characterize the superficial and painted layers of the samples and to further support the investigations conducted by XRF and SEM-EDX. Moreover, GC-MS technique was used for a preliminary investigation of the used binders.

As a matter of fact, the relevance of the investigation carried out is expressed by the fact that it made possible to attest and confirm what is generally believed by the art historians, that hypothesize the use by Mattia Preti of only a few primary pigments, unlike his pupils who used a much more complex palette to create a composite pictorial film made up of several layers and a mix of various colors. It is a research of absolute novelty, in which pigments play a key role in recognizing, within a given painting, the hand of the master and, therefore, in distinguishing it from that of his many collaborators, especially in the last 20 years of the painter's life.

Along with a detailed diagnostic investigation of the materials composition, the 3D digitalization of the masterpiece allowed us to highlight, for the first time on a painting by Mattia Preti, the unevenness of the original surfaces as well as the presence of layers subsequently applied during the various restoration interventions.

It is worth underlying that the knowledge of all the aforementioned aspects does not simply constitute a fundamental pre-requisite in view of the development of proper restoration strategies to be applied. As a matter of fact, being the composition of the grounds of Italian painters of the 17th century, such as Mattia Preti, connected to the place where the artwork was realized (Hradil et al. 2020), the identification of the source materials represents the groundwork for dating and locating the *St. Michael defeating Evil* painting to a specific period of the artist's productive life, i.e., in Italy or in Malta. This is, at present, an ongoing controversy among the scientific and humanities community, also considering the close relation between these two regions.

Materials and methods

Materials and sampling

Overall, 12 points were investigated, *in situ* and in the laboratory (see Fig. 2).

In particular, as far as laboratory analyzes are concerned, 11 micro-fragments of the pictorial surface (size smaller than ~ 5 mm^2) were sampled from the edge of already-existing lacunae, in proximity of aging-induced surface cracks, during the latest restoration intervention in 2019. This allows the characterization of the pictorial technique as well as of overlapping layers on the painting. Details about sampling are described in Table 1, together with all the analytical techniques employed.

It is worth underlying that the sampling procedure was conducted following minimal invasiveness principles, and taking into account that the painting under investigation was, at the time, in an advanced state of deterioration.

In this sense, the identification of colors by visual inspection turned out to be a very challenging task.

In situ analysis: XRF technique and 3D digital survey

XRF spectra were collected through a portable XRF "Alpha 4000" (Innov-X system) analyzer, which allowed the detection of chemical elements having an atomic number (Z) between phosphorus and lead. The instrument was equipped with a Ta anode X-ray tube excitation source, and a Si PIN diode detector with an active area of 170 mm^2. The apparatus operated using a Compton Normalization algorithm ("soil" mode), designed for achieving the lowest Limit of Detection (LOD) possible (trace concentrations, from levels of ppm) for soil and bulk samples. The "soil" mode was here adopted together with the "Environmental" elements suite. For the used "soil" mode, the following element list was used: P, S, Cl, K, Ca, Ti, Cr, Mn, Fe, Co, Ni, Cu, Zn, As, Se, Br, Rb, Sr, Zr, Mo, Ag, Cd, Sn, Sb, I, Ba, Au, Hg, and Pb. For each analyzed area, two sequential tests were carried out. In particular, the working conditions were 40 kV and 7 μA for the first one and, 15 kV and 5 μA for the second one, for a total collection time of 120 s (60 s per run). A Hewlett-Packard iPAQ Pocket PC was used to manage the instrument and as data storage. The calibration was carried out by soil LEAP (Light Element Analysis Program) II and was verified using alloy certified reference materials produced by Analytical Reference Materials International. Lines detected at ~ 8.15 keV and ~ 9.34 keV, observed for all the investigated samples, were attributed to the L_α and L_β energy transition of Ta anode.

Concerning the 3D survey, the final 3D model was obtained (Fig. 3) by applying the processing and workflow described in (Colica et al. 2018) and (D'Amico et al. 2017). More in detail, the photogrammetric survey was carried out through the employment of a Sony Alpha RIII camera equipped with a 35 mm lens. In order to reconstruct the model of Fig. 3, ~ 400 images were acquired. For the sampling distance points, we used a local coordinate system and we deployed a number of control points located near the painting. This allows to properly scale the final digital model and to obtain a high accuracy in the measurements.

After the fine mesh geometry generation and reconstruction, the model was textured and used also for the development of a high-resolution (0.226 mm/pixel) orthomosaic. Finally, a Digital Elevation Model (DEM) of the surface was generated. The same process was applied also to images acquired using ultra-violet (UV) light and a different digital

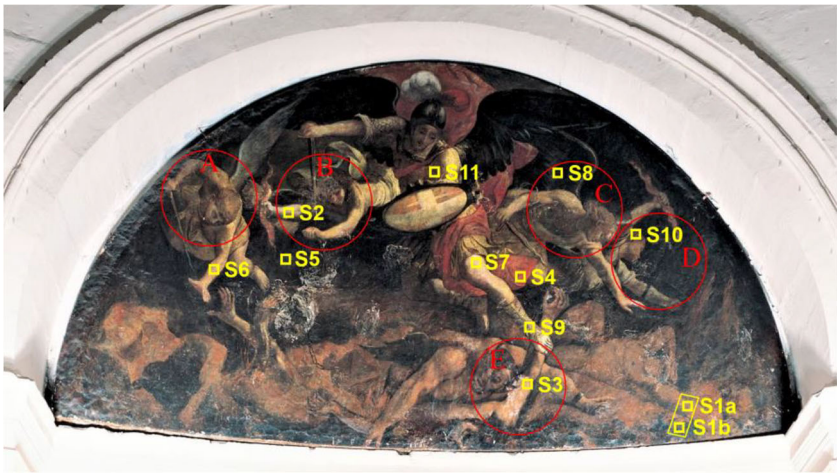

Fig. 2 Analyzed points from the *St. Michael defeating Evil* painting. Red circles account for the position of the four angels (**A-D**) and the devil (**E**)

model of the painting was generated (Fig. 3a). An accurate 3D model of the frame was also obtained (Fig. 3b).

Both 3D digital Red-Green-Blue (RGB) (Fig. 3c-d) and UV (Fig. 3a) models were inspected for a first visual analysis, and different filters were applied in order to improve the contrast between the different areas and parts of the painting. In particular, the use of the UV orthophoto, coupled with some information gathered during the physical survey, allowed to discriminate regions potentially covered by the original painting or subsequent restorations. A 3x3 filter was firstly applied to the referenced and measurable 3D RGB model, in order to smooth the DEM with the main goal of eliminating noisy points that generate a false rugose texture. After this step, we applied a typical set of procedures that are usually employed to derive accurate digital elevation models. In this context, the high-resolution of the 3D model and the accurate measurements allowed us to apply this technique, mainly used for large scale objects, such as topographic profiles at different scales, contour maps, hill shading visualization, and 3D visualization, in the field of archaeometry, where it is not widely

Table 1 Investigated samples, description and techniques employed

Sample ID	Description	Techniques employed[b]
S1a[a]	Bottom, right-side of the canvas, *Light area*	XRF
S1b	Bottom, right-side of the canvas, *Dark area*	XRF, SM, SEM-EDX, FT-IR
S2	Right arm of the angel on the left (B), *Brown-gray*	SM, SEM-EDX, FT-IR
S3	Right arm of the devil (E), *Uncertain color tending to brownish-bluish*	SM, SEM-EDX, FT-IR, GC-MS
S4	Cloak of *St. Michael*, *Red*	XRF, SM, SEM-EDX, FT-IR
S5	Angel wing on the left (A), *Black*	XRF, SM, SEM-EDX, FT-IR
S6	Incarnate of the angel on the left (A), *Beige*	SM, SEM-EDX, FT-IR
S7	Incarnate of *St. Michael*, *Uncertain color tending to beige-grayish*	SM, SEM-EDX, FT-IR, GC-MS
S8	Angel wing on the right (C), *Blackish-brownish*	XRF, SM, SEM-EDX, FT-IR
S9	Sandalwood of *St. Michael*, *Green-yellowish*	XRF, SM, SEM-EDX, FT-IR
S10	Hair of the angel on the right (D), *Uncertain color tending to brownish*	SM, SEM-EDX, FT-IR
S11	*St. Michael*'s armor, *Uncertain color tending to beige-grayish*	SM, SEM-EDX, FT-IR

[a] Unfortunately, due to practical difficulties, the sampling of micro-fragment S1a was not possible. Accordingly, only *in-situ* XRF spectroscopy was carried out.

[b] When more than one technique is employed, measurements were carried out on the same sample.

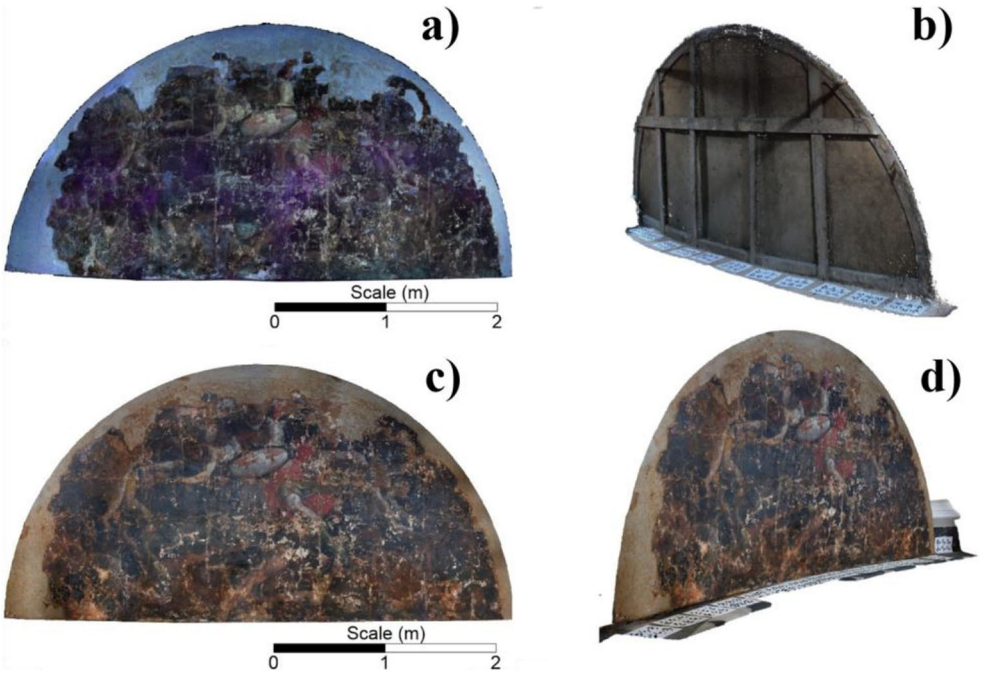

Fig. 3 3D photogrammetric reconstruction of the *St. Michael defeating Evil* painting. **a** Model reconstructed using the UV light, **b** 3D model of the painting frame, **c** orthophoto, and **d** 3D model obtained using the RGB pictures

diffused. This approach allowed us to obtain a very good representation of the topographic variations spanning from the millimetric to the metric scale and gave us the possibility to identify topographic alignments as well as to map other morphologic features. An *ad hoc* Geographic Information System (GIS) environment was generated and the DEM, the RGB and UV orthophotos were imported. In such a way, mainly using the DEM and the UV orthophotos as a further digital support, we generated polygons delimitating the different canvasses and the restored parts on the RGB orthophoto. We also were able to map the principal alignments generated by topographic variations, color variations or a combination of both.

Laboratory analysis: SM, SEM-EDX, FT-IR, and GC-MS techniques

Stereomicroscopic investigations were conducted to closely examine the cross sections of the samples, and were carried with a Zeiss Axiolab microscope equipped with a digital camera to capture images. Observations allowed to highlights the structure of the samples, i.e., the stratigraphy and the overlapping of the various and subsequent layers.

SEM-EDX analyzes were performed on the surface of the samples (both on the back and on the front of the fragments) to obtain information about the micromorphology and chemical composition (in terms of major elements). Analyzes were performed with a scanning electron microscope Hitachi TM4000, equipped with a detector STEM. Microanalysis was performed using an energy dispersive spectrometer EDX Oxsford -AztecOne. Analyzes were carried out with an acceleration voltage of 5 kV, 10 kV e 15 kV and under high vacuum conditions.

As far as FT-IR investigation is concerned, the used spectrophotometer was a Perkin Elmer Spectrum 100, equipped with an attenuated total reflectance (ATR) accessory. Infrared spectra were recorded in ATR mode, in the 500–4000 cm^{-1} wavenumber range, with a resolution of 4 cm^{-1}. Due to the complexity of the FT-IR absorbance profiles, the samples' spectra were also compared with those of standard minerals and/or pigments from databases (Vahur et al. 2016) and literature (Derrick et al. 2000) for a reliable assignment of the bands.

The determination of the organic binding media was carried out by means of gas chromatography/mass (GC-MS) technique using a GC-MS_TQ8040NX instrument (Shimadzu). He was the carrier gas (1mL/min) and separation was achieved by a capillary column VF-5ms (26 m × 0.25 mm i.d. × 0.25 μm). The sample (1μL) was introduced into the column by splitless injection with the following temperature program: 100°C for 2 min, 6°C/min up to 280°C, and finally 280°C for 10 min. Mass spectra were recorded in full-scan mode in the 50–1000 amu m/z range. Sample preparation was achieved following a consolidated procedure reported in the literature (Colombini et al. 1999); briefly the microfragment underwent a clean-up procedure by NH_3, followed by an acid hydrolysis by HCl 6M and a subsequent derivatization by BSTFA. The fatty acids and the amino acids detected and analyzed were those reported in the literature (Casoli et al. 1996; Colombini et al. 1998, 1999).

Results and discussion

XRF analysis

XRF measurements on six different areas of the Lunette were carried out (Fig. 2, Table 1) in order to identify the elemental composition of superficial layer. Specifically, spectra were collected from points S1a and S1b, respectively, associated to a light and a dark area of the canvas (the surface paint layer was, in these points, locally damaged), and from points S4, S5, S8, and S9, corresponding to red (S4), black (S5 and S8), and green-yellowish (S9) pigmented areas. The obtained elemental composition of the aforementioned areas is summarized in Table 2, whereas the obtained spectra, with the exception of spectrum of sample S8, that almost completely matched the spectrum of sample S5, are reported in Fig. 4.

A first inspection of Fig. 4a reveals, for both S1a and S1b points, the detection of S (K_α and K_β transition lines at ~ 2.31 keV and ~ 2.46 keV, respectively), Ca (K_α and K_β transition lines at ~ 3.68 keV and ~ 3.99 keV, respectively), Pb (L_α and L_β transition lines at ~ 10.55 keV and ~ 12.61 keV, respectively), and Fe (K_α and K_β at ~ 6.40 keV and ~ 7.05 keV, respectively). Their simultaneous presence suggests that the investigated surface can be attributed to a Ca-based and S-based preparatory layer, probably made of calcium carbonate ($CaCO_3$) and gypsum ($CaSO_4{\cdot}2H_2O$) or burnt gypsum (anhydrite, $CaSO_4$), mixed with a Fe-based compound, probably ochre (Fe_2O_3), lightened by a Pb-based compound, that could be lead white ($2PbCO_3{\cdot}Pb(OH)_2$), according to what reported in literature regarding Mattia Preti's execution technique (Chiavari et al. 2007; Pelosi et al. 2018; Ridolfi 2019; Hradil et al. 2020; D'Amico et al. 2021).

Moreover, being "oil on canvas" the painting technique used by Mattia Preti for the realization of the panel, the use of a Pb-based compound as dryer for the binder could be also reasonably hypothesized (Venuti et al. 2020). It is worth underlying that although sample S1b appeared, during the measurement acquisition, of an intense darkish-brownish coloration, the XRF spectrum collected on this area did not reveal any components attributable to pigmenting agents capable to offer dark shades/tonalities. The brownish color clearly visible to the naked eye could therefore, be due to naturally-occurring transformation processes of the original portion of the canvas into newly-formed mineral phases, consequently, the prolonged exposure of the painting to the surrounding environment. In particular, the simultaneous detection of high amount of Pb and S (see Table 2) can be considered as an indication of the presence of alteration products based on lead sulfide (galena, PbS), originating from the interaction between atmospheric hydrogen sulfide (H_2S, arising from pollution) and the investigated portion of the canvas. In fact, the production of PbS, characterized by an intense blackish-brownish coloration and an extremely low solubility, must be attributed to the reaction of H_2S with the Pb^{2+} ions of the pictorial surface, resulting in a visible blackening of the corresponding region (Smith and Clark 2002; Coccato et al. 2017). It is worth of note that the acidic nature of the H_2S mainly favors the aforementioned reaction with materials consisting of basic substances, such as the $Pb(OH)_2$ units in lead white, supporting our hypothesis concerning the presence of such compound in the material composition of the S1b area.

In addition, the exposition of lead-based compounds with oxidizing or biodeteriogenic agents (*fungi*) can favor the production of lead dioxide (plattnerite, PbO_2) onto the topmost pictorial layer of the painting, especially when a combination of alkaline and high humidity conditions occurs (Burgio et al. 2001). The so-formed mineral, being a low-soluble inorganic dark-brown solid, strongly affects the readability of the original polychrome, contributing to the brown discoloration observed, by visual inspection, in sample S1b.

In the case of the red area (Fig. 4b), the detected chemical elements suggested the use of Hg-/Fe-based compounds, indicating that a mixture of cinnabar/vermilion (HgS) and red ochre was probably employed. In addition, the simultaneous detection of Pb and Ti allows us to reasonably hypothesize the use of a mixture of Pb-based pigments, having red, such as minium (Pb_3O_4), and white, such as lead white, coloration, respectively. They seem to be mixed with a poor amount of a Ti-based compound (according to the corresponding relative intensity observed for Pb and Ti peaks), such as titanium dioxide (TiO_2), a modern white pigment, in order to obtain red/reddish tonalities, as those found in the bottom part of the analyzed cloak (see Fig. 2).

For what concerns the investigated black areas (S5 and S8), a comparable elemental composition can be observed (see Table 2), suggesting the employment by Mattia Preti of a similar receipt for the blackish-brownish tonalities. More in detail, the observation of high intensity peaks (Fig. 4c) at ~ 3.68 keV and ~ 3.99 keV, respectively, ascribed to the K_α and K_β transition lines of Ca, indicates the use of a carbon-based blackish pigment of organic nature, containing calcium, in agreement with previous published papers regarding Mattia

Table 2 Elemental composition, as obtained by XRF data, of the analyzed points. The key elements for pigment identification are marked in bold. The minor or trace elements are presented in parentheses

Point of analysis	XRF elemental composition
S1a	Ca, S, Pb, (Cl, Fe, K, Zn, Sr, Ba)
S1b	S, Ca, Pb, Cl, Fe, (As, K, Ba, Zn)
S4	S, Pb, Cl, As, **Fe**, Ca, K, **Hg**, (Sn, Cd)
S5	Ca, S, As, Fe, Pb, (Sr, Sb, Mn)
S8	S, Ca, Pb, As, Fe, (Sb, Mn, Sr)
S9	S, Ca, Pb, K, (**Fe**, As, Sb, Ba, Zn, Mn)

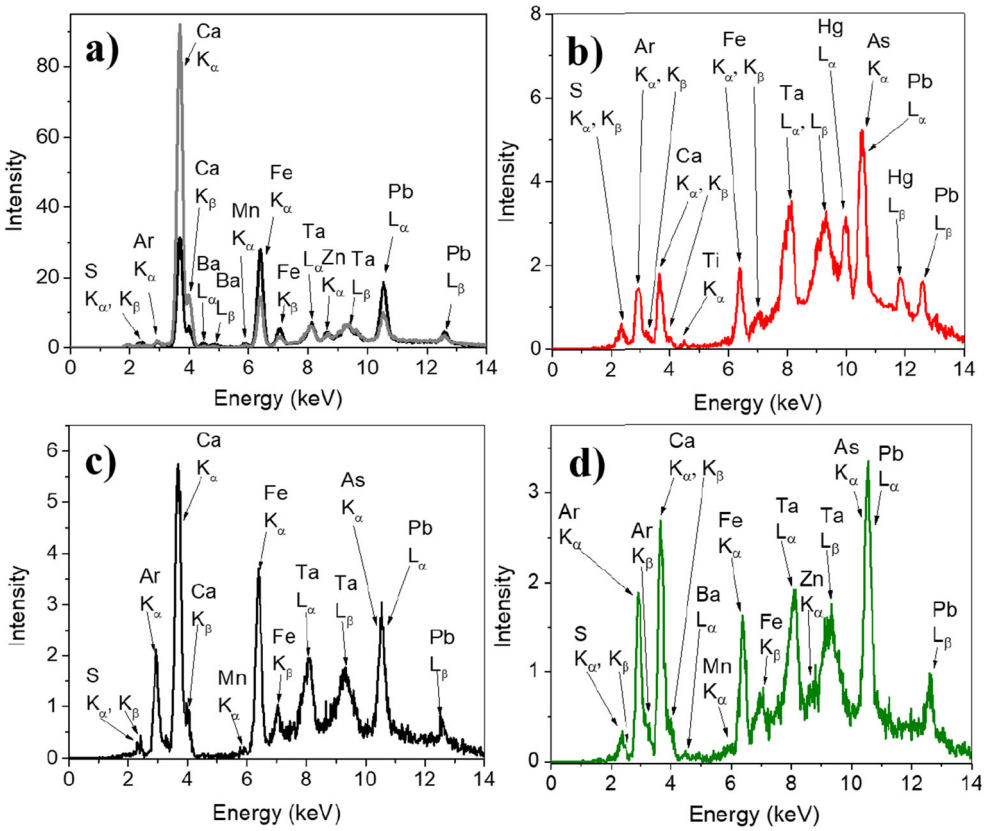

Fig. 4 XRF spectra, in the 0-14 keV range, collected on **a** the light (point S1a, gray line) and dark (point S1b, black line) area on the right-side of the canvas, **b** the red cloak of *St. Michael* (point S4, red line), **c** the black wing of the angel on the left side of the painting (point S5, black line), and **d** the green-yellowish sandalwood of *St. Michael* (point S9, green line)

Preti's palette (Chiavari et al. 2007; Pelosi et al. 2018; Ridolfi 2019; Hradil et al. 2020; D'Amico et al. 2021). It could be either bone black (~ 20% of elemental carbon and the remaining ~ 80% consisting of hydroxyapatite), commonly obtained by charring animal bones in a low oxygen environment, or ivory black (~ 20% of elemental carbon and the remaining ~ 80% consisting of a mixture of calcium phosphate and calcium carbonate), usually attained by charring ivory from animal tusks and/or teeth. It is worth of note that the vine black, traditionally obtained by charring wood or plants, is also fully compatible with the elemental composition observed for the S5 and S8 areas. At the same time, the application of a C/Ca-based compound such as asphalt black, made up of a mixture of organic (bitumen), and inorganic (carbonates and calcium oxides) components, cannot be excluded. It is reasonable to assume that this black pigmenting agent was also applied as color background for other dark areas of the Lunette, including the entire upper-section of the painting, the *St. Michael*'s helmet and the wings of the angels. In this case, however, no further information can be obtained by means of XRF spectroscopy, since the characteristic elements of such compound have a low Z number. Nevertheless, the simultaneous detection of traces of Fe and Mn suggests that the organic black pigment was probably mixed with natural umber (Fe_2O_3 + MnO_2 + nH_2O + Si + Al_2O_3), a common Fe/Mn-based dark-brownish pigment.

As far as the XRF spectrum of the green-yellowish area is concerned (Fig. 4d), the detection of the characteristic XRF transition lines of Fe and Pb indicates the application of a common Fe-based green pigment, mixed, even in this case, with a Pb-based white compound (possibly lead white) in order to obtain different shades/nuances. Going on, the observation of traces of Sb (see Table 2), in conjunction with Pb, suggests the possible addition in the mixture of a Pb/Sb compound, probably Naples yellow, in order to obtain the observed yellowish nuance. Worth of note, the experimental XRF spectrum of the green-yellowish area did not reveal any contribution related to Cu, which leads us to exclude the use of a Cu-based green pigmenting agent in the painting, although frequently applied at that time.

For all the investigated areas, the presence of Ba and Zn, when detected, indicates the possible application of modern synthetic compounds, probably ascribed to previous restoration interventions (Feller 1986).

Finally, the presence of a significant amount of Ca in all the investigated areas deserves clarifications. In fact, this occurrence supports the hypothesis regarding the presence of the typical globigerina limestone in the preparatory layer of the painting (Hradil et al. 2020), whose observation appears crucial in order to ascribe the investigated painting to the Maltese period of the artist. However, confirmation of this statement needs the endorsement of complementary methodologies,

being the distinction among different chemical compounds by XRF analysis not possible.

Stereomicroscopic analysis

Stereomicroscopic investigations were conducted to closely examine the cross sections of the sampled micro-fragments (see Fig. 5).

Sample S1b is completely impregnated, which makes the stratigraphy unclear with the exception of the most superficial layer that appears of brownish color. Nevertheless, given the strong sample impregnation and translucent appearance probably due to the use of different compounds (e.g., glues) in previous restoration interventions, it is not clear whether the dark layer can be related to an alteration or to a superficial pictorial film. Sample S2 is also impregnated, but shows three overlapping layers that, from the surface toward the inside, appear brownish, blackish, and reddish in color, respectively. Sample S3 is the only one with a clearer stratigraphy and four visible layers. From the surface inwards, it is possible to distinguish a layer with blue pigments, followed by a whitish layer, a blackish layer and a reddish one. Sample S4 shows three clearly visible layers, which, from the surface inwards, range from a red layer, to a blackish layer and a reddish one in

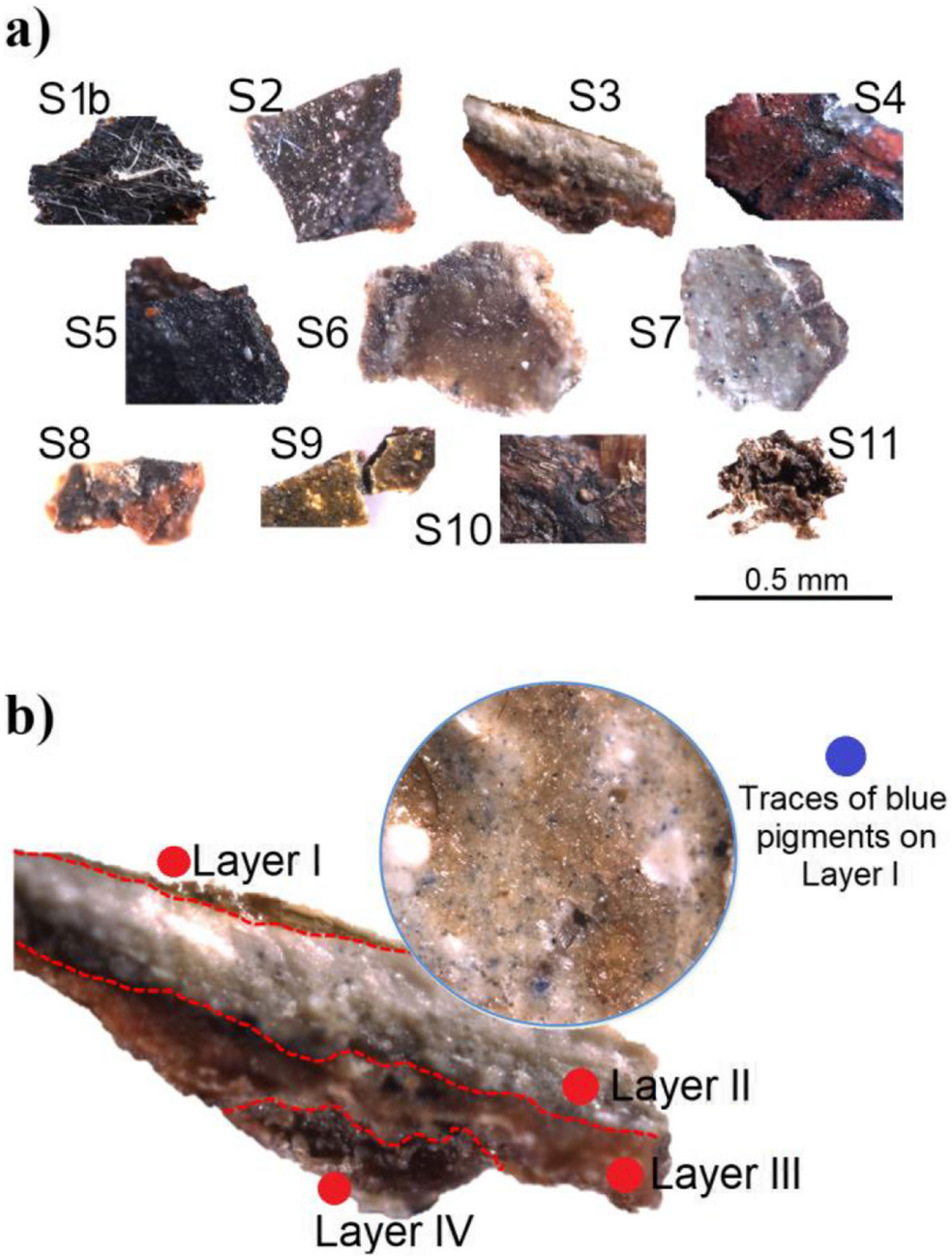

Fig. 5 **a** Images by stereomicroscope of the sampled micro-fragments; **b** Representative stratigraphy of micro-fragment S3

the lower portion. Samples S5–S9 are all strongly impregnated samples with unclear stratigraphy, for which only the superficial pictorial layer is clearly visible. Specifically, S5 shows a pictorial blackish layer, S6 beige, S7 whitish-beige, S8 brownish-blackish, and S9 green-yellowish. Regarding samples S10 and S11, they are also strongly impregnated, the stratigraphy is not delineated and, furthermore, the painted surface layer is not visible.

SEM-EDX analysis

SEM-EDX investigations were conducted on 11 microfragments (see Table 1), investigating both the pictorial layer and the underlying. A summary of the data is reported in Table 3, where the elemental composition of the painting surfaces is shown for each analyzed sample.

EDX analyzes can provide information on the artist's technique for the creation of the canvas, as well as they can identify the presence of elements that could be associated to restorations carried out in the past.

As for the composition of the layers under the painting film, for almost all samples the presence of Ca, Pb, and Fe prevails (Table 3). Such composition clearly suggests that the preparatory layer could contain species linked to these elements, such as calcium carbonate, lead white, and red ochre (Fig. 6a-c). These data are in agreement with the findings coming from the XRF survey. Furthermore, it is worth to note that several studies report the use of such compounds during the Maltese period of Mattia Preti (Lalli et al. 2014; Pelosi et al. 2018; D'Amico et al. 2019; Ridolfi 2019).

For some fragments, as in the case of sample S1b, it was possible to investigate the stratigraphy (Fig. 6d-i), only in terms of composition, acquiring EDX maps in false colors. The maps better highlighted the artist's execution technique and the application of the preparation layer on the canvas. The data acquired suggested that: a) the layer in contact with the canvas has a composition mainly based on Ca and Fe; b) the layer below the pictorial film shows the presence of Pb and S. The use of pigments such as lead white, ochre and calcium carbonate could be hypothesized. Furthermore, the presence, even if in low concentration, of Al, K, and Si (Table 3) is detected. These elements are compatible with the presence of alunite ($KAl_3(SO_4)2(OH)_6$) and silicates, commonly used by the artist for the preparatory layers of his paintings on canvas (Hradil et al. 2020). Further morphological observations by SEM, carried out in more detail on the layer in contact

Table 3 Summary of EDX elemental (weight %) analyzes for all the samples

		O	Ca	Si	S	Na	Mg	Al	Pb	Fe	Ba	Zn	Cl	P	K	Hg	Sb	Mn
layer underneath the paint film	**Sample S1b**	29.79	52.55	0.97	2.03	0.44	0.30		10.29	1.40			0.83	0.40	1.00			
	Sample S2	33.65	45.19	8.16	3.69	1.79	1.18	1.92	31.99	2.16				0.27	1.99			
	Sample S4	33.24	34.01	5.64	4.06	2.60		5.21	11.64	1.00				1.10	1.50			
	Sample S6	33.32	48.58	5.19	2.77	2.60	0.52	1.39	2.44	1.80			0.37	0.42	0.60			
	Sample S8	35.30	29.86	12.92	1.43	1.20	0.82	2.29	6.44	7.50			0.47	0.47	1.30			
	Sample S10	30.68	34.64	3.00	4.16	3.77	0.53	1.47	5.59	5.55	5.65	1.96	0.73	0.58	1.69			
	Sample S11	30.20	30.32	3.18	4.64	3.68	0.96	1.62	6.57	3.97	8.37	2.00	1.64	0.68	2.17			
pictorial film	**Sample S1**	27.20	24.37	2.96	4.36	1.10	0.31	1.45	23.28	5.67	4.21	2.92	1.04	0.76	0.37			
	Sample S2	31.90	18.03	2.99	6.21	0.63	3.08	1.44	22.07	3.09	3.92	3.92	1.44	0.71	0.57			
	Sample S3	29.99	34.15	0.93		0.48	0.61	0.85	22.99	10.00								
	Sample S4	19.88	8.54	1.23	15.72	1.31	0.22	0.95	20.90	0.79		0.43	0.53		2.14	27.36		
	Sample S5	36.15	34.73	3.04	4.05		0.72	1.01	18.20						2.11			
	Sample S6	20.55	22.30	5.84	3.85	0.86	0.34	3.04	33.91	3.54	2.66	1.14	0.63	0.28	1.06			
	Sample S7	20.70	24.01	5.73	5.72	0.58	1.00	3.24	33.88	3.81			0.50		0.83			
	Sample S8	18.57	11.25	3.49	1.54	1.01	0.34	1.25	57.58	2.65	0.75			0.47	1.10			
	Sample S9	24.64	13.55	3.82	5.54	1.52	0.99	0.61	38.93	2.66	2.91		1.12		3.71			
	S9 white particles	18.88		0.54	6.06	0.37		0.25	36.97	0.83			1.08		6.80		28.23	
	Sample S10	28.21	29.83	6.30	3.46	2.12	0.60	2.43	10.13	7.32	3.15	1.48	0.91	0.69	1.98			1.39
	Sample S11	29.51	27.08	7.16	2.45	2.25	0.89	3.45	11.25	8.04	1.94	1.16	0.69	0.89	1.75			1.49

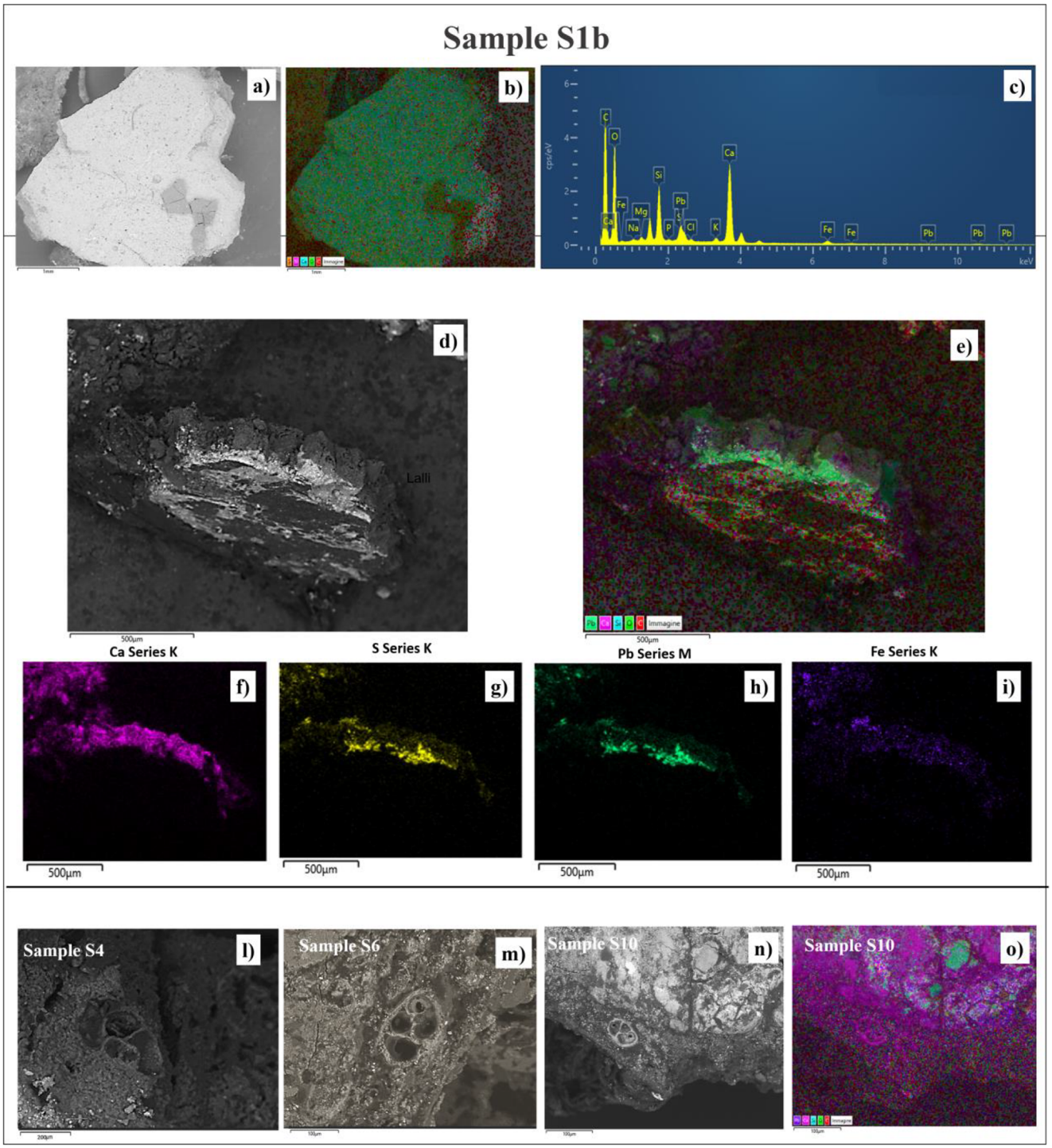

Fig. 6 SEM images showing the layers below the pictorial film of some samples. **a** Back-Scattered Electrons (BSE) image of sample S1b (scale bars 1mm); **b** SEM-EDX false-color map obtained from the analysis of the surface of sample S1b (scale bars 1mm); **c** EDX spectrum obtained from the analyzed surface of sample S1b (scale bars 500 µm), **d** BSE image of sample S1b placed vertically to the painting surface (scale bars 500 µm); **e** SEM-EDX false-color map obtained from the analysis of the surface of sample S1b placed vertically to the sampled surface (scale bars 500 µm); **f** SEM-EDX false color map of Ca (scale bars 500 µm); **g** SEM-EDX false color map of S (scale bars 500 µm); **h** SEM-EDX false color map of Pb (scale bars 500 µm); **i** SEM-EDX false color map of Fe (scale bars 500 µm); **l** BSE image of globigerina observed in sample S4 (scale bars 200 µm); **m** BSE image of globigerina observed in sample S6 (scale bars 100 µm); **n** BSE image of globigerina observed in sample S10 (scale bars 100 µm); **o** SEM-EDX false color map of sample S10 where globigerina was observed (scale bars 100 µm)

with the canvas, highlighted the presence of foraminifera and in particular of the genus globigerina (Fig. 6l-n), with typical calcitic composition (Fig. 6o). The foraminifera represent the fingerprint of the artist's Maltese production, deriving from

the use of the local globigerina limestone that Mattia Preti used to accentuate the red color for the preparation layer of his paintings. According to the literature (Pelosi et al. 2018; D'Amico et al. 2019), Mattia Preti preferred the red color of the soil made by microfossiliferous limestones, adding gypsum, alunite, opal, silicates, hematite, and lead white.

As regards sample S2, the EDX investigations on the pictorial layer showed a high Pb content, thus allowing us to hypothesize the use of a lead white also as a pigmenting agent and not only for the preparatory layer of the canvas.

In the case of samples S3, S5, and S8, it was not possible to hypothesize specific pigments, in agreement with what already observed for samples S5 and S8, by XRF analysis. In fact, according to the observations by stereomicroscope, the pictorial surfaces showed a blue color for the sample S3, a brown-blackish color for sample S5, and a black color for sample S8. It is known that Mattia Preti used pigments such as carbon black, vine black, bone black (Chiavari et al. 2007; Lalli et al. 2014; Pelosi et al. 2018; Hradil et al. 2020) for the black color, and blue glaze, indigo or lapis (Chiavari et al. 2007; Pelosi et al. 2018; Ridolfi 2019) for blue pigments. Nevertheless, the elements indicative of the presence of these pigments were not highlighted.

As for the sample S4, that appeared red when observed under the stereomicroscope, the EDX analyzes showed high concentrations of S, Hg, Pb, and Ca (Table 3, Fig. 7), which suggest the use of cinnabar/vermilion, as also hypothesized by XRF analysis, and of minium, both pigments used together in the palette of Mattia Preti to paint red surfaces (Chiavari et al. 2007; Pelosi et al. 2018). On sample S4, EDX maps were acquired in false colors (Fig. 7a-f), confirming that the entire surface is composed of the aforementioned elements. Further investigations, by performing an EDX analysis following a linear trajectory along the sample surface (Fig. 7g), revealed similar profiles of Hg (series M) and S (series K), confirming the presence of HgS. On the contrary, the profiles of Ca (K series) and Pb (M series) appear different, suggesting that lead is present on the surface as a pigment different from lead white (probably minium).

Samples S6 and S7, taken from two different areas of the incarnates, respectively, those of the angel on the left of the canvas (S6) and from *St. Michael* (S7), show an almost similar chemical composition of the pictorial layer with high concentrations of Pb and Ca and lower quantities of Si, Al, and Fe. The chemical composition detected by EDX suggests, on the basis of the elements characteristic of the corresponding pigments, the use of a mixture composed of lead white added to red lead and green earth, pigments used by Mattia Preti to reproduce a skin color (Lalli et al. 2014), although the use of green earth cannot be confirmed in this study. The only difference in the chemical composition of S6 and S7 (Fig. 8) is the presence of low concentrations of Ba and Zn (Table 3), the latter found only in S6 (and also in other samples as reported in Table 3).

The presence of Ba and Zn on the pictorial surface in some specific points confirms that the canvas underwent restoration work in the past. In fact, these two elements can be due to the use of zinc white (ZnO) and barium white ($BaSO_4$) or to the

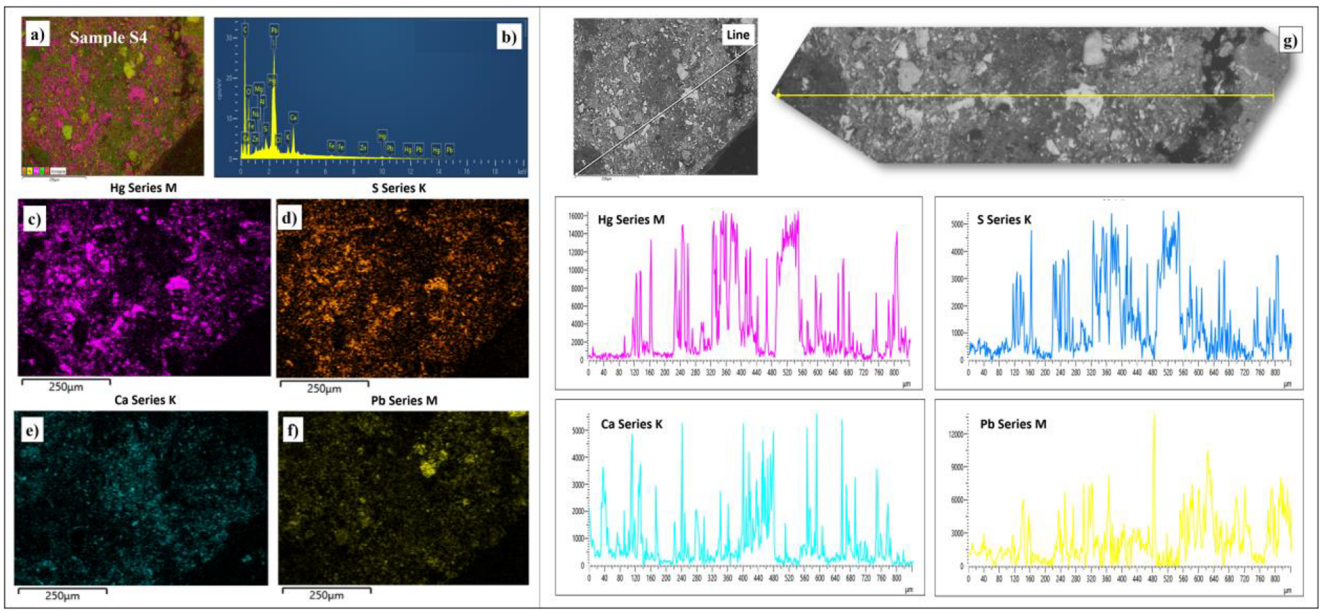

Fig. 7 SEM-EDX images showing the analysis of sample S4. **a** SEM-EDX false-color map obtained from the analysis of the surface of sample S4 (scale bars 250 µm), **b** EDX spectrum obtained from the analyzed surface of sample S4, **c** SEM-EDX false-color map of Hg (scale bars 250 µm), **d** SEM-EDX false-color map of S (scale bars 250 µm), **e** SEM-EDX false-color map of Ca (scale bars 250 µm), **f** SEM-EDX false-color map of Pb (scale bars 250 µm), **g** EDX analysis following a linear trajectory performed on the surface of sample S4 (scale bars 250 µm), with associated profilometry spectra of Hg, S, Ca, and Pb

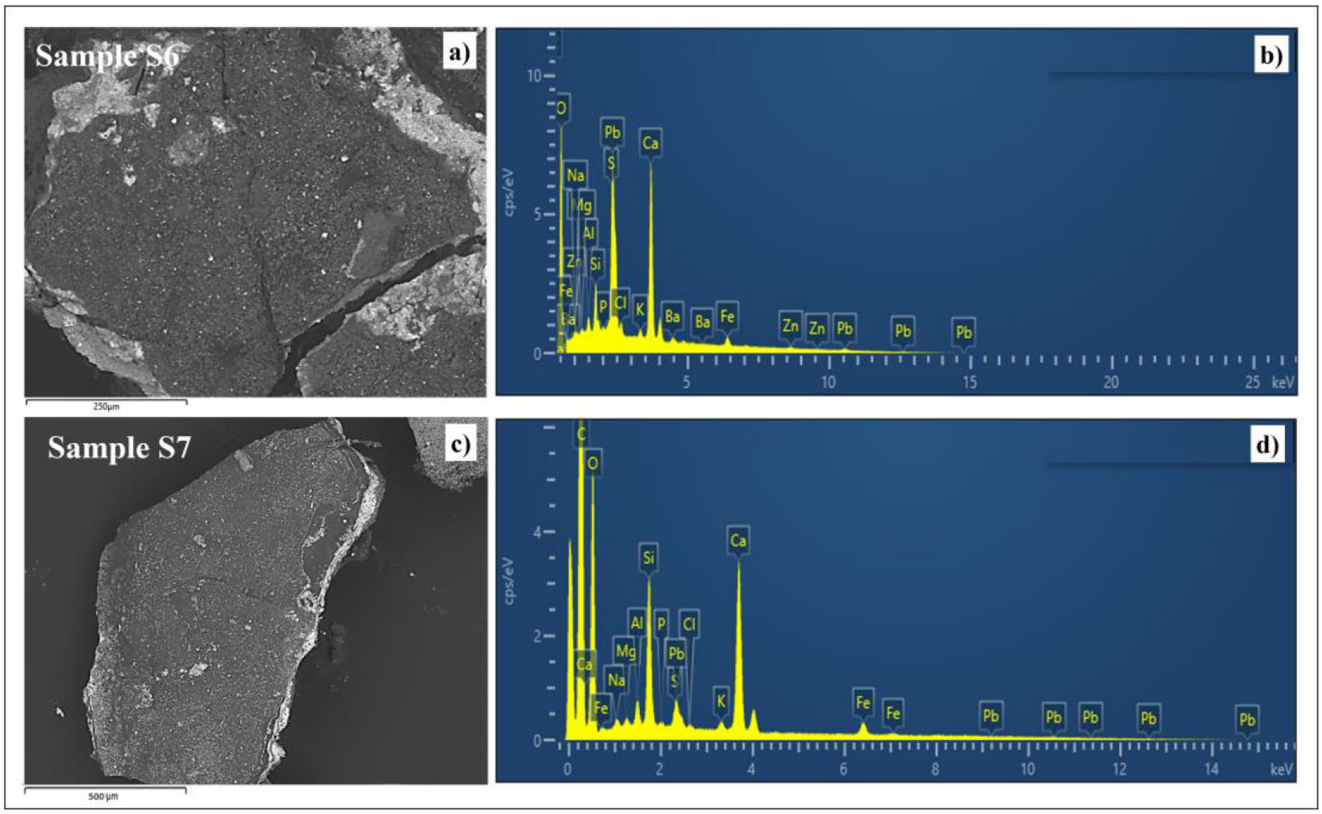

Fig. 8 SEM- EDX images showing the analysis of sample S6 and S7. **a** BSE image of sample S6 (scale bars 250 μm), **b** EDX spectrum obtained from the analyzed surface of sample S6, **c** BSE image of sample S7 (scale bars 500 μm), **d** EDX spectrum obtained from the analyzed surface of sample S7

use of lithopone, i.e., a white composed of barium sulfate and zinc sulfide ($BaSO_4$ + ZnS), pigments produced since the end of the 19th century.

As for the EDX analysis performed on the sample S9, it allowed us to support the hypothesis of the use of Naples yellow pigment, also known as "Giallo d'Antimonio", among the most used yellow pigments in Mattia Preti's palette (Ridolfi 2019; Hradil et al. 2020), as already suggested by the XRF composition collected on the same point. In this regard, Pb and Sb were, in particular, detected (Table 3) on single particles, such as that shown in Fig. 9a, whose EDX spectrum is reported in Fig. 9b. Interestingly, low amount of Fe can be recognized, in agreement with XRF results, indicating the possible addition of a Fe-based pigment in order to obtain different green-yellowish shades/nuances.

Lastly, the brownish colored samples S10 and S11, as evidenced by the observations under stereomicroscope, show a similar elemental composition. In particular, high concentrations of Ca and Pb (Table 3) were detected, followed by Al, Si, and Fe, and low concentrations of Mn. The results suggest the use of Sienna, a color composed of iron oxides, clay silicates and small amount of manganese dioxide, probably mixed with lead white.

FT-IR analysis

Infrared spectroscopy was essentially addressed at characterizing the main inorganic materials (i.e., mineralogical phases) within the samples. All the analyzes are referred to the whole sample, since it was not possible to isolate the surface from the bulk and the various layers, nor was the sample ground, given its very small size, fragility, and the risk of completely losing the material. Some representative spectra are reported in Fig. 10.

In all analyzed samples, the stretching vibrations of calcite, peaked at ~ 1409, ~ 875 and ~ 711 cm^{-1} were identified (Derrick et al. 2000; Vahur et al. 2016), supporting the thesis that the artist used the globigerina limestone, the typical oligo-Miocene limestone of Malta, in the preparatory layers. This thesis can be further confirmed as in some samples (i.e., samples S6 and S9) aragonite (i.e., a polymorph of calcium carbonate) has been identified (peaks at ~ 1788, ~ 1473, ~ 1082, ~ 906, ~ 854, ~ 712, and ~ 699 cm^{-1}) (Linga Raju et al. 2002), as a consequence of the dissolution of calcium carbonate skeletal fragments and typical of the skeletal structures of organisms such as foraminifera (globigerina). Overall, calcite and aragonite have to be considered as aggregates used for the

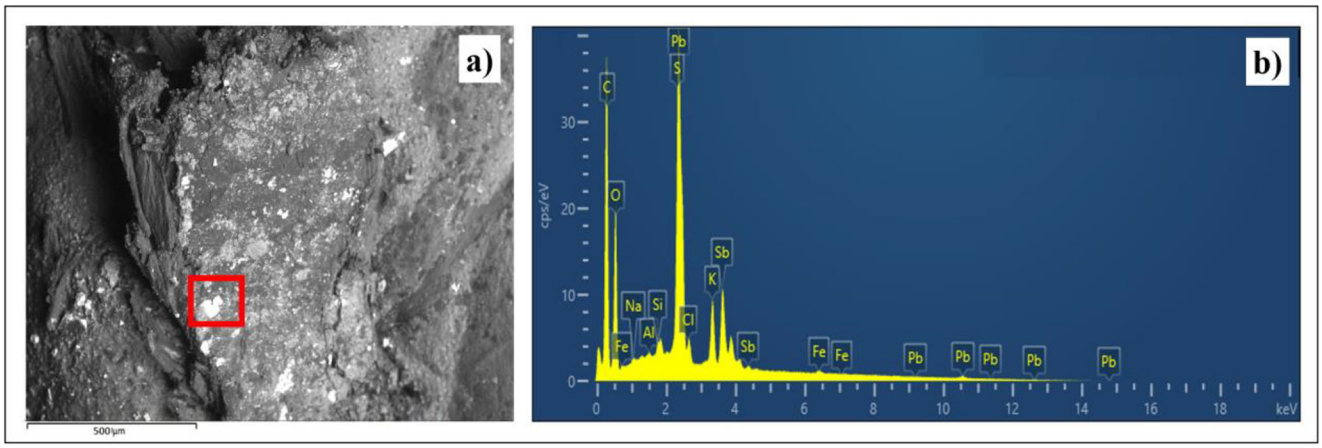

Fig. 9 SEM-EDX images showing the analysis of sample S9 white particles. **a** BSE image of an area of sample S9 (scale bars 500 μm) (the red rectangle indicates the analyzed area), **b** EDX spectrum obtained from the analyzed area

realization of the preparatory layer, being the matrix mainly composed by calcium carbonates, as also suggested by the SEM-EDX analysis. Of course, both phases may also have been used as white pigments; based on the fact that aragonite was often used in association with cinnabar/vermilion in order to "dilute" the red color, or with other pigments to tone down

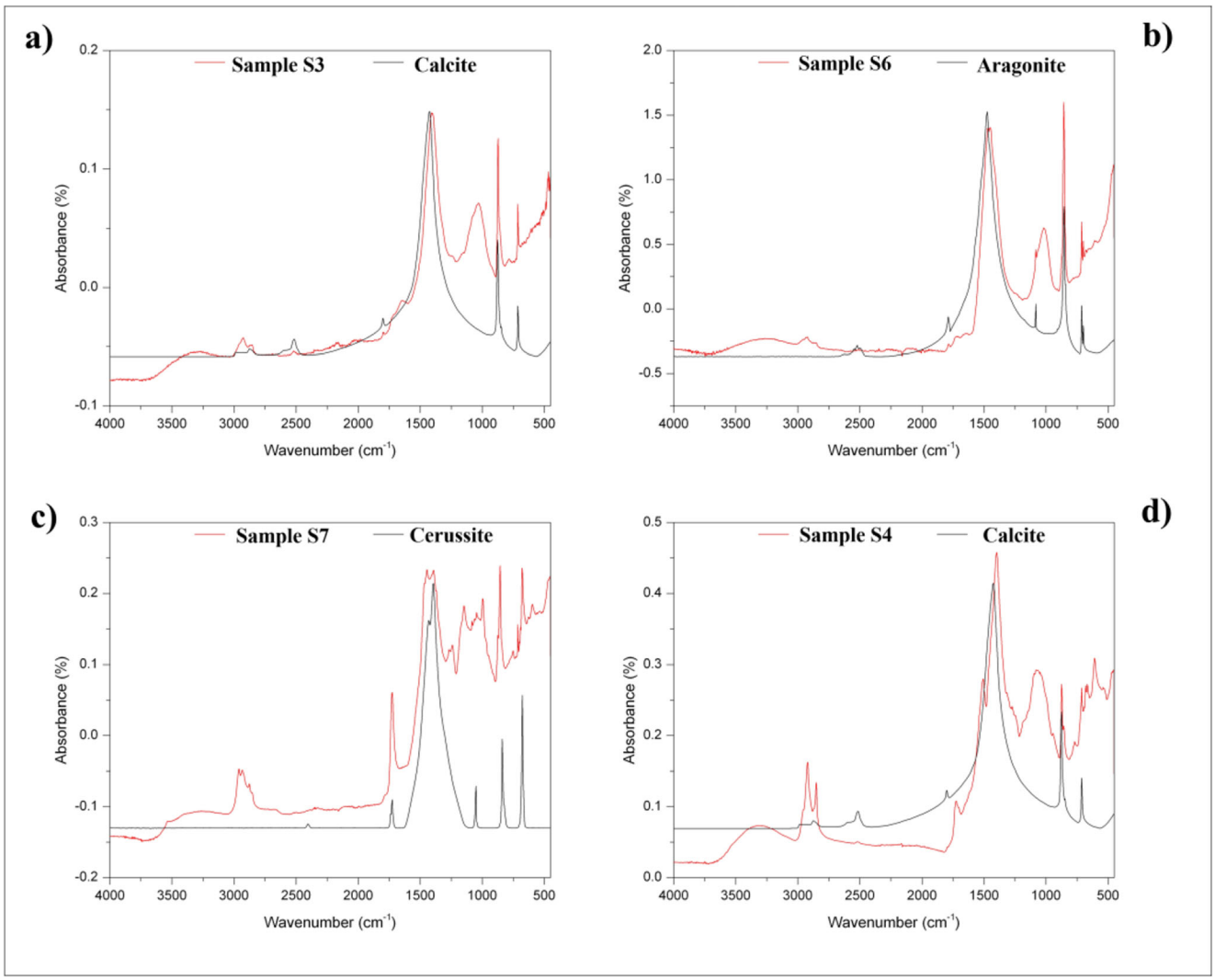

Fig. 10 Representative FT-IR absorbance spectra of the **a** S3, **b** S6, **c** S7, and **d** S4 samples

the color and to dose the shade, or to prepare a white base (Angelini et al. 2019).

The absorbance band, which is strong in all the samples, peaked at ~ 1020 cm^{-1} is ascribable to the stretching of Si–O bond, indicating silicate compounds, probably deriving from sandy raw materials used as inert in the preparatory layers or as pigmenting agent.

The presence of cerussite (i.e., lead carbonate, $PbCO_3$) was also detected in sample S7, with typical peaks at ~ 1432, ~ 1394, ~ 1051, ~ 838, and ~ 677 cm^{-1}. It is indicative of the probable use of lead white, one of the most widely used white pigments in the past, mainly because of its high opacity and hiding power (Learner 2007; de Viguerie et al. 2018; Gonzalez et al. 2019).

Finally, taking into account the hypothesis deduced from the XRF and SEM-EDX investigations, regarding samples S6, S7, and S9, no bands attributable to green earth have been identified.

In addition to inorganic compounds, samples showed the stretching bands of the carboxylic (−COOH) group peaked at ~ 1700 cm^{-1}, particularly evident in sample S7, and those of the stretching of C–H group at ~ 2852 and ~ 2922 cm^{-1}, suggesting the presence of organic matter which is probably highly related to the binder. In the case of sample S4, the band at ~ 1700 cm^{-1} is present together with a band at ~ 1510 cm^{-1} that could be due to the amide group (Fermo et al. 2020), or also to the presence of some carboxylate group possibly coming from alteration of carboxylic acids in the binder. The third typical amide band is at ~ 1440 cm^{-1}, but it is masked by the carbonate signal, so it cannot be highlighted.

GC-MS analysis

GC-MS analyzes were carried out only on samples S3 and S7. Both fatty acids and amino acids were detected in these two samples. It is worth nothing that in case of sample S3 the signal at ~ 1700 cm^{-1} was very weak and it was not possible to distinguish other signals (such as the bands due to amide group), while for sample S7 the presence of the very intense signal due to cerussite in the same region of the absorption bands typical of the amide group didn't allow to evidence other absorptions. For this reason, GC-MS analysis represents a valuable method for the precise identification of specific organic binders.

Thanks to the comparison with reference values reported in the literature (Casoli et al. 1996; Colombini et al. 1998, 1999), the presence of linseed oil and animal glue were disclosed in these two samples. The identification of these binders was carried out through the construction of a correlation matrix that higlilighted high values of correlation coefficients (> 0.85) with reference samples containing these two binders. The animal glue was probably present in the preparatory layer underneath the painting film, while the siccative oil was employed as binder. This is in accordance with what already found for other paintings by Mattia Preti (Chiavari et al. 2007).

This preliminary study deserves further investigation by expanding the number of samples.

3D photogrammetric survey

Three different canvasses, as well as the areas that experienced previous restorations, were identified and mapped. Each of these areas has characteristic features, as "geographic" distribution, topographic position, texture, RGB range of colors, and response to the UV light (Fig. 11a). Canvas 1 represents the canvas where the original paint is located. It has a central position in the painting and, clearly, presents restored parts. The restored part represents the restoration stucco, used to complete the missing parts of the Canvas 1 (Fig. 11b, c). It is interesting to see how these restored parts (which represent parts where the original paint was damaged) have got lineal patrons. Canvas 2 is a canvas under the Canvas 1 and used in a previous and old restoration phase. Presumably, the actual total size of this canvas is bigger than the Canvas 1, but it is covered by it, so the exposed area is relatively small. Canvas 3 lies under Canvas 1 and Canvas 2, in contact with the latter. As Canvas 2, most of its area is covered, and it is well exposed in the borders of the painting. Table 4 shows the size of the total and the visible areas of the different canvasses, extracted from the GIS analysis.

During the analysis of the reconstructed 3D digital model, it was possible to recognize on the painting different kinds of alignments (Fig. 11d). These parts are different in color, texture and topographical features. In light blue we marked a horizontal line approximately in the middle of the painting. This line is pointing an alignment affecting just the Canvas 1. It is interpreted as a merging feature within the Canvas 1. The upper light blue dashed line (inferred position) is located parallel to the first one and separated by about 1.20 m. In this region, Canvas 1 is not visible, thus we located the potential position of the merged canvasses taking into account the position of the main join, as well as the size of the typical canvas at the time of Mattia Preti available in Malta and southern Italy. The green line is interpreted as an internal union of the Canvas 2. This union is very evident and directly visible, and it does not affect either Canvas 1 or Canvas 3. The lines in red are placed where the original painting was damaged, and we interpreted them as a weakness line. They are distributed both in the horizontal and vertical directions. We interpret those features as sign of folding of the painting. In fact, historical fonts report that the painting has been folded a couple of times, the last one during the Second World War, when the painting was stored away and kept in a safe place. The folding was done probably first in the horizontal direction, and then the

Table 4 Results extracted from GIS analysis

	Total area (sq m)	Total area (%)	Visible area (sq m)	Visible area (%)
Canvas 3	8.39	100	1.38	16.47
Canvas 2	7.01	83.53	2.35	28.01
Canvas 1	4.66	55.52	2.85	33.99
Restored	1.81	21.53	1.81	21.53
Restored area in relation with Canvas 1 (%)	38.78			

painting was rolled, causing the damage in the vertical direction.

The morphological analysis (Fig. 12) revealed the external "U" shape of the Lunette, being flatted on the boarder. This "U" shape is less evident near to the top of the painting. The difference between the highest part on the edges and lowest part on the low center of the painting turned out to be 28 cm. The construction of the frame following this shape was necessary in order to accommodate the painting in its present location. This analysis, together with the 3D model (Fig. 3), will allows to print the frame with exactly the same features and measurements in case of any damage to the structure. The high resolution DEM also allowed us to do observations at more detailed scale. At millimetric scale, it was possible to discriminate among the three different canvasses and to determine the thickness of the Canvas 1, between 1 and 1.5 mm, with a relatively thick paint layer, and of the Canvas 2, equal to 1 mm, without any paint.

Finally, during the restoration a thermal camera was used to monitor the application of consolidants (Fig. 13) used to strengthen the painting. In particular, different injection points of such consolidating media were revealed, identified as the

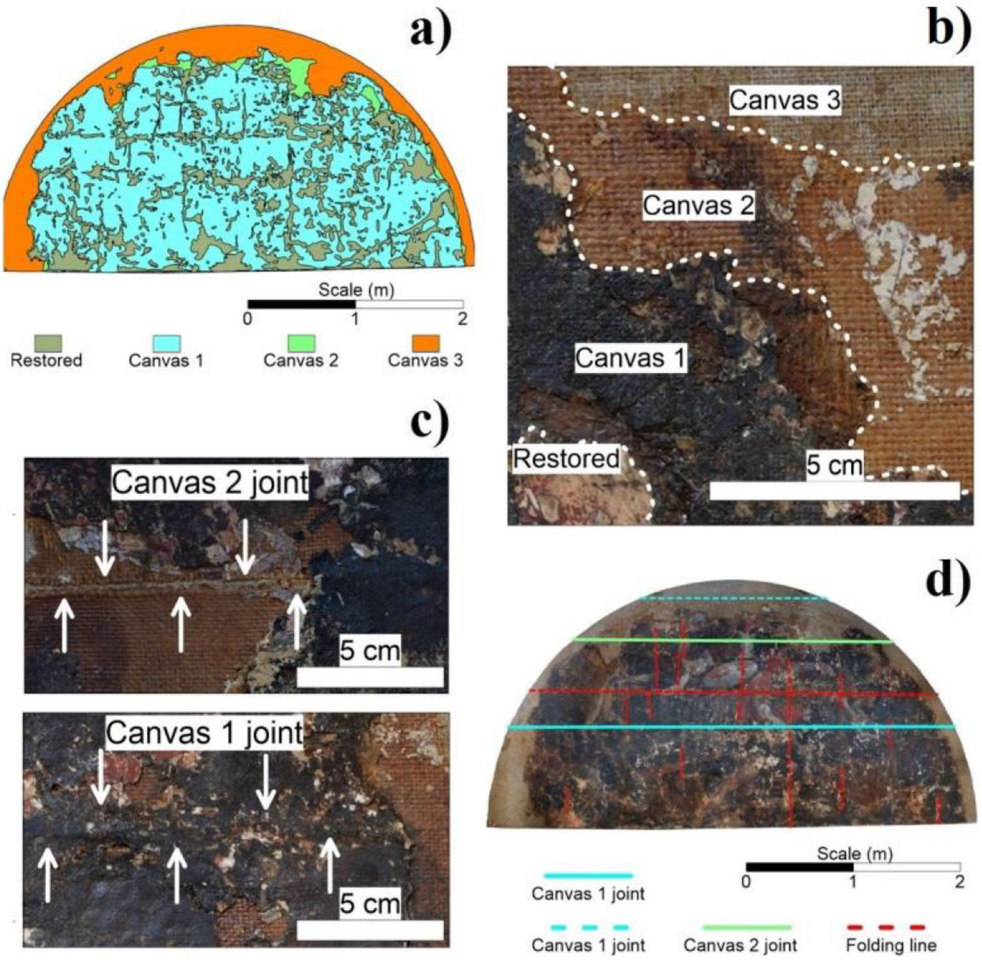

Fig. 11 Results of the interpretation obtained using the digital 3D model. **a** Mapping of the three different canvasses and restored areas. Panels **b-d** show details of the painting highlighting the different types of canvas as well as the joints between them

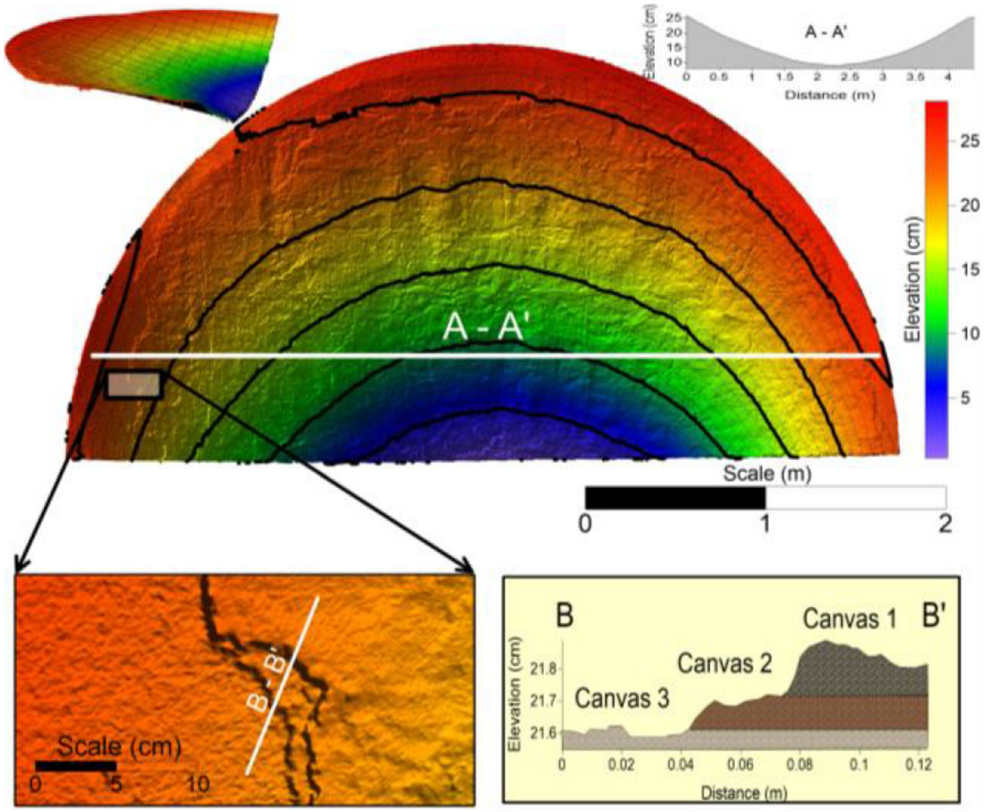

Fig. 12 Reconstructed DEM of the painting. The top panel shows the high precision model of the entire artifact as well as its curvature. Bottom panel shows a detail of the model where the 3 different canvasses can be identified; the sketch on the right reports a schematic reconstruction

dark spots/areas in thermal images. In the future, such kind of approach can be used in real-time to monitor each phase of the restoration work with the aim of optimizing the timing of the different phases.

Concluding remarks

In the present work, a combined approach involving noninvasive optical and physical/chemical analysis, ranging from elemental to molecular scale, and 3D digital survey, was successfully applied on the large *St. Michael defeating Evil* painting by Mattia Preti, located inside the Church of the Immaculate Conception of Sarria (Floriana) in Malta. Table 5 summarizes all the analytical techniques employed in this study, together with the main results achieved.

In particular, the combined use of XRF, SEM-EDX, FT-IR, and GC-MS techniques allowed us to identify, starting from the evaluation of elemental/molecular compositions, the pigmenting agents, preparatory. and organic binding materials used by the artist, so providing a better understanding of the execution technique, the artist's palette and the occurrence of nondocumented restoration treatments. In this context, random interventions were testified by the detection of

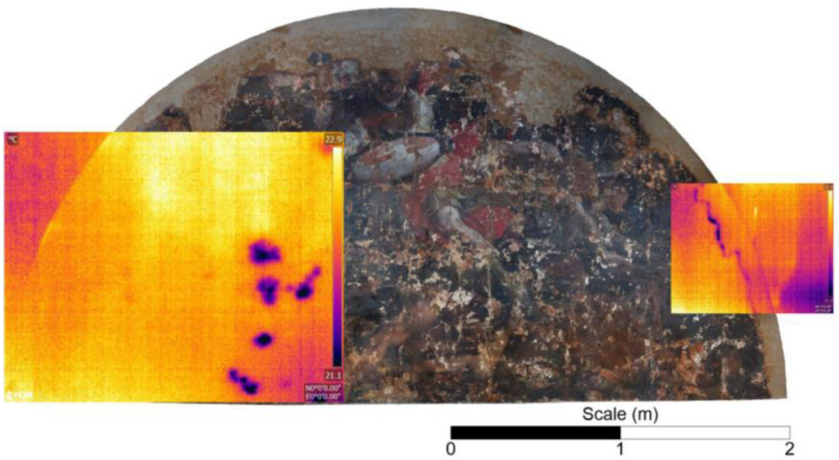

Fig. 13 Thermal image of the painting during the restoration

Table 5 Techniques employed and main results achieved

Techniques employed	Results/conclusions achieved
In situ analysis	
XRF	Characterization of the elemental composition of both the pictorial layer and underlying stratifications—better understanding of the Mattia Preti execution technique—identification of modern/synthetic pigments—evidence of nondocumented restoration interventions.
3D photogrammetric survey	Morphological variations spanning from the millimetric to the metric scale—extension of damaged parts—mapping of the domains of the different canvasses employed.
Laboratory analysis	
SM	Characterization of the sample structure—stratigraphy—overlapping of the various and subsequent layers.
SEM-EDX	Characterization of the elemental composition of both the front and back of sampled fragments—evaluation of the micromorphology—identification of modern/synthetic pigments—evidence of nondocumented restoration interventions.
FT-IR	Identification of mineralogical phases—molecular characterization of the superficial painted layers—use by Mattia Preti of the typical Maltese globigerina limestone (from the identification of both calcite and, for same samples, aragonite)
GC-MS	Preliminary characterization of the used binders—use of animal glue in the preparatory layer and of siccative oil as binders.

elements generally associated to modern/synthetic media. In addition, measurements allowed us to confirm, among other aspects, the use by Mattia Preti of the typical Maltese globigerina limestone as main component for the painting ground, furnishing an experimental evidence of the Maltese origin of the investigated painting. This also contributes to temporally locate the investigated Lunette to the Maltese period of the artist, which was, up to now, still unverified. On the other side, the obtained 3D digital models of the painting allowed us to quantify the extension of damaged parts, to map the domains of the different canvasses employed, to derive its state of conservation and to highlight possible additions made during previous nondocumented restorations. These aspects, along with the characterization of the materials through complementary methodologies, are essential in order to optimize the restoration project and to safeguard the materials through time. The knowledge of the chemical/physical characteristics of the constituent materials of the work of art, accompanied by noninvasive imaging investigation for an in-depth view of the state of conservation, represents a fundamental pre-requisite in order to select the best cleaning, consolidation, integration, and protection phases of the restoration process. As a matter of fact, a lack of analytical data on materials and on decay products can lead to improper restoration choices.

Acknowledgements The authors are grateful to Dr. Mattia Casanova and Shimadzu Italia srl for the support in GC-MS analysis. The authors kindly acknowledge Dr. Massimo Tagliaferro and Nanovision S.r.l. (Italy) for the scientific support and for having provided us with the Hitachi TM-4000 instrument.

Availability of data and materials All data generated or analyzed during this study are included in this published article. All the metadata related to the photogrammetric survey and results are available on request.

Authors' contribution S. D'Amico, S. Guido, G. Mantella, V. Venuti performed sampling. S. D'Amico, E. Colica, and L. Galone carried out the 3D photogrammetric survey. V. Comite, P. Fermo carried out SEM-EDX and GC-MS investigation. G. Paladini, V. Crupi, D. Majolino, V. Venuti carried out XRF investigation. M. Ricca, M. F. La Russa, L. Randazzo carried out stereomicroscopic analysis and FT-IR investigation. S. Guido, G. Mantella provided all information regarding the historic-artistic context. S. D'Amico, V. Comite, G. Paladini, M. Ricca, and V. Venuti wrote the manuscript. All authors read and approved the final manuscript.

Declarations

Ethics approval and consent to participate Not applicable.

Consent for publication Not applicable.

Competing interests The authors declare no competing interests.

References

Aicardi I, Chiabrando F, Maria Lingua A, Noardo F (2018) Recent trends in cultural heritage 3D survey: the photogrammetric computer vision approach. J Cult Herit 32:257–266. https://doi.org/10.1016/j.culher.2017.11.006

Angelini I, Asscher Y, Secco M, Parisatto M, Artioli G (2019) The pigments of the frigidarium in the Sarno Baths, Pompeii: identification, stratigraphy and weathering. J Cult Herit 40:309–316. https://doi.org/10.1016/j.culher.2019.04.021

Arias P, Armesto J, Di-Capua D, González-Drigo R, Lorenzo H, Pérez-Gracia V (2007) Digital photogrammetry, GPR and computational

analysis of structural damages in a mediaeval bridge. Eng Fail Anal 14:1444–1457. https://doi.org/10.1016/j.engfailanal.2007.02.001

Armesto J, Arias P, Roca J, Lorenzo H (2008) Monitoring and assessing structural damage in historic buildings. Photogramm Rec 23:36–50. https://doi.org/10.1111/j.1477-9730.2008.00466.x

Balletti C, Beltrame C, Costa E, Guerra F, Vernier P (2016) 3D reconstruction of marble shipwreck cargoes based on underwater multi-image photogrammetry. Digit Appl Archaeol Cult Herit 3:1–8. https://doi.org/10.1016/j.daach.2015.11.003

Barbera G, Barone G, Crupi V, Longo F, Majolino D, Mazzoleni P, Sabatino G, Tanasi D, Venuti V (2012) Study of Late Roman and Byzantine glass by the combined use of analytical techniques. J Non Cryst Solids 358:1554–1561. https://doi.org/10.1016/j.jnoncrysol.2012.04.013

Bersani D, Lottici PP, Casoli A, Cauzzi D (2008) Pigments and binders in "Madonna col Bambino e S. Giovannino" by Botticelli investigated by micro-Raman and GC/MS. J Cult Herit 9:97–102. https://doi.org/10.1016/j.culher.2007.05.005

Bersani D, Berzioli M, Caglio S, Casoli A, Lottici PP, Medeghini L, Poldi G, Zannini P (2014) An integrated multi-analytical approach to the study of the dome wall paintings by Correggio in Parma cathedral. Microchem J 114:80–88. https://doi.org/10.1016/j.microc.2013.11.014

Burgio L, Clark RJH, Firth S (2001) Raman spectroscopy as a means for the identification of plattnerite (PbO2), of lead pigments and of their degradation products. Analyst 126:222–227. https://doi.org/10.1039/b008302j

Casoli A, Musini PC, Palla G (1996) Gas chromatographic-mass spectrometric approach to the problem of characterizing binding media in paintings. J Chromatogr A 731:237–246. https://doi.org/10.1016/0021-9673(95)01194-3

Castro K, Ábalos B, Martínez-Arkarazo I, Etxebarria N, Madariaga JM (2008) Scientific examination of classic Spanish stamps with colour error, a non-invasive micro-Raman and micro-XRF approach: the King Alfonso XIII (1889-1901 "Pelón") 15 cents definitive issue. J Cult Herit 9:189–195. https://doi.org/10.1016/j.culher.2008.02.001

Chelazzi D, Bordes R, Giorgi R, Holmberg K, Baglioni P (2020) The use of surfactants in the cleaning of works of art. Curr Opin Colloid Interface Sci 45:108–123. https://doi.org/10.1016/j.cocis.2019.12.007

Chiavari G, Prati S, Lanterna G, Lalli C, Cagnini A (2007) Diagnostic study of the materials and painting techniques in "The Dinner of Emmaus" by Gregorio (and Mattia?) Preti. Microchim Acta 159:357–362. https://doi.org/10.1007/s00604-007-0759-2

Coccato A, Moens L, Vandenabeele P (2017) On the stability of mediaeval inorganic pigments: a literature review of the effect of climate, material selection, biological activity, analysis and conservation treatments. Herit Sci 5:12. https://doi.org/10.1186/s40494-017-0125-6

Colica E, Micallef A, D'Amico S, Cassar LF, Galdies C (2018) Investigating the use of UAV systems for photogrammetric applications: a case study of Ramla Bay (Gozo, Malta). J Malta Chamb Sci 5:125–131. https://doi.org/10.7423/XJENZA.2017.2.04

Colombini MP, Fuoco R, Giacomelli A, Muscatello B (1998) Characterization of proteinaceous binders in wall painting samples by microwave-assisted acid hydrolysis and GC-MS determination of amino acids. Stud Conserv 43:33. https://doi.org/10.2307/1506634

Colombini MP, Modugno F, Giacomelli A (1999) Two procedures for suppressing interference from inorganic pigments in the analysis by gas chromatography–mass spectrometry of proteinaceous binders in paintings. J Chromatogr A 846:101–111. https://doi.org/10.1016/S0021-9673(99)00192-2

Comite V, Ricca M (2016) Diagnostic investigation for the study of the fresco "Madonna con il bambino", from Cosenza, southern Italy: a case study. Rend Online della Soc Geol Ital 38:21–24. https://doi.org/10.3301/ROL.2016.07

Crupi V, Fazio B, Fiocco G, Galli G, La Russa MF, Licchelli M, Majolino D, Malagodi M, Ricca M, Ruffolo SA, Venuti V (2018) Multi-analytical study of Roman frescoes from Villa dei Quintili (Rome, Italy). J Archaeol Sci Reports 21:422–432. https://doi.org/10.1016/j.jasrep.2018.08.028

D'Amico S, Saccone M, Persico R, Venuti V, Spagnolo GV, Crupi V, Majolino D (2017) 3D survey and GPR for cultural heritage. The case study of SS. Pietro and Paolo Church in Casalvecchio Siculo. Kermes 107:11–15

D'Amico S, Venuti V, Colica E, Crupi V, Majolino D, Paladini G, Guido S, Mantella G, Zumbo R (2019) Scientific investigation of the Conversion of St Paul painting (Mdina, Malta). In: 2019 IMEKO TC-4 International Conference on Metrology for Archaeology and Cultural Heritage. pp 330–334

D'Amico S, Venuti V, Colica E, Paladini G, Galone L, Crupi V, Majolino D, Guido S, Mantella G (2020) Digital reconstruction and scientific analysis prior the restoration of two paintings by Mattia Preti in the Church of the Immaculate Conception of Sarria (Floriana, Malta). In: 2020 IMEKO TC-4 International Conference on Metrology for Archaeology and Cultural Heritage. pp 532–537

D'Amico S, Venuti V, Colica E, Crupi V, Paladini G, Sante G, Mantella G, Majolino D (2021) A combined 3D surveying, XRF and Raman in-situ investigation of The Conversion of St Paul painting (Mdina, Malta) by Mattia Preti. ACTA IMEKO 10:173–179 https://doi.org/10.21014/acta_imeko.v10i1.824

de Viguerie L, Glanville H, Ducouret G, Jacquemot P, Dang PA, Walter P (2018) Re-interpretation of the Old Masters' practices through optical and rheological investigation: the presence of calcite. Comptes Rendus Phys 19:543–552. https://doi.org/10.1016/j.crhy.2018.11.003

Derrick MR, Stulik D, Landry JM (2000) Infrared spectroscopy in conservation science. Getty Publications

Edwards HGM, Jorge Villar SE, Eremin KA (2004) Raman spectroscopic analysis of pigments from dynastic Egyptian funerary artefacts. J Raman Spectrosc 35:786–795. https://doi.org/10.1002/jrs.1193

Feller RL (1986) Barium sulfate—natural and synthetic. In: Artists' pigments: a handbook of their history and characteristics. pp 47–64

Fermo P, Mearini A, Bonomi R, Arrighetti E, Comite V (2020) An integrated analytical approach for the characterization of repainted wooden statues dated to the fifteenth century. Microchem J 157:105072. https://doi.org/10.1016/j.microc.2020.105072

Fiorillo F, Jiménez Fernández-Palacios B, Remondino F, Barba S (2015) 3d Surveying and modelling of the Archaeological Area of Paestum, Italy. Virtual Archaeol Rev 4:55. https://doi.org/10.4995/var.2013.4306

Gonzalez V, Wallez G, Calligaro T, Gourier D, Menu M (2019) Synthesizing lead white pigments by lead corrosion: new insights into the ancient manufacturing processes. Corros Sci 146:10–17. https://doi.org/10.1016/j.corsci.2018.10.033

Hradil D, Hradilová J, Lanterna G, Galeotti M, Holcová K, Jaques V, Bezdička P (2020) Clay and alunite-rich materials in painting grounds of prominent Italian masters—Caravaggio and Mattia Preti. Appl Clay Sci 185:105412. https://doi.org/10.1016/j.clay.2019.105412

La Russa MF, Ruffolo SA, Belfiore CM, Comite V, Casoli A, Berzioli M, Nava G (2014) A scientific approach to the characterisation of the painting technique of an author: the case of Raffaele Rinaldi. Appl Phys A 114:733–740. https://doi.org/10.1007/s00339-013-7866-1

Lalli CG, von Breska-Ficović N, Innocenti F, Kolić Pustić M (2014) Le due serie dei quattro "Evangelisti" di Mattia Preti a Dubrovnik: un progetto multidisciplinare e di collaborazione tra il Laboratorio Scientifico dell'Opificio e l'Istituto Croato di RestauroSource: OPD Restauro. Cent Di Della Edifimi SRL 26:231–248

Learner T (2007) Modern paints: uncovering the choices. In: Modern paints uncovered: proceedings from the modern paints uncovered symposium

Linga Raju C, Narasimhulu K, Gopal N, Rao J, Reddy BC (2002) Electron paramagnetic resonance, optical and infrared spectral studies on the marine mussel Arca burnesi shells. J Mol Struct 608:201–211. https://doi.org/10.1016/S0022-2860(01)00952-8

Pelosi C, Agresti G, Baraldi P (2018) The 'slash of light' in the late religious paintings of Mattia Preti technique and materials. Eur J Sci Theol 14:151–160

Remondino F (2011) Heritage recording and 3D modeling with photogrammetry and 3D scanning. Remote Sens 3:1104–1138. https://doi.org/10.3390/rs3061104

Remondino F, Girardi S, Rizzi A, Gonzo L (2009) 3D modeling of complex and detailed cultural heritage using multi-resolution data. J Comput Cult Herit 2:1–20. https://doi.org/10.1145/1551676.1551678

Ricca M, Paladini G, Rovella N, Ruffolo SA, Randazzo L, Crupi V, Fazio B, Majolino D, Venuti V, Galli G, La Russa MF (2019) Archaeometric characterisation of decorated pottery from the archaeological site of Villa dei Quintili (Rome, Italy): preliminary Study. Geosciences 9:172. https://doi.org/10.3390/geosciences9040172

Ridolfi S (2019) Relazione tecnico-scientifica delle indagini effettuate sull'Allegoria dei cinque sensi di Mattia e Gregorio Preti

Rosi F, Burnstock A, Van den Berg KJ, Miliani C, Brunetti BG, Sgamellotti A (2009) A non-invasive XRF study supported by multivariate statistical analysis and reflectance FTIR to assess the composition of modern painting materials. Spectrochim Acta Part A Mol Biomol Spectrosc 71:1655–1662. https://doi.org/10.1016/j.saa.2008.06.011

Ruffolo SA, La Russa MF, Barca D, Casoli A, Comite V, Nava G, Crisci GM, De Francesco AM, Miriello D (2010) Mineralogical, petrographic and chemical analyses for the study of the canvas "Cristo alla Colonna" from Cosenza, Italy: a case study. Period di Mineral 79:71–79. https://doi.org/10.2451/2010PM0022

Smith GD, Clark RJH (2002) The role of H2S in pigment blackening. J Cult Herit 3:101–105. https://doi.org/10.1016/S1296-2074(02)01173-1

Tschegg C, Ntaflos T, Hein I (2009) Integrated geological, petrologic and geochemical approach to establish source material and technology of Late Cypriot Bronze Age Plain White ware ceramics. J Archaeol Sci 36:1103–1114. https://doi.org/10.1016/j.jas.2008.12.004

Vahur S, Teearu A, Peets P, Joosu L, Leito I (2016) ATR-FT-IR spectral collection of conservation materials in the extended region of 4000-80 cm–1. Anal Bioanal Chem 408:3373–3379. https://doi.org/10.1007/s00216-016-9411-5

Venuti V, Fazzari B, Crupi V, Majolino D, Paladini G, Morabito G, Certo G, Lamberto S, Giacobbe L (2020) In situ diagnostic analysis of the XVIII century Madonna della Lettera panel painting (Messina, Italy). Spectrochim Acta Part A Mol Biomol Spectrosc 228:117822. https://doi.org/10.1016/j.saa.2019.117822

Vizárová K, Reháková M, Kirschnerová S, Peller A, Šimon P, Mikulášik R (2011) Stability studies of materials applied in the restoration of a baroque oil painting. J Cult Herit 12(2):190–195. https://doi.org/10.1016/j.culher.2011.01.001

Wolbers R (2000) Cleaning Painted Surfaces: Aqueous Methods. Archetype Publications Ltd, London ISBN: 1 873132 360

Yilmaz HM, Yakar M, Gulec SA, Dulgerler ON (2007) Importance of digital close-range photogrammetry in documentation of cultural heritage. J Cult Herit 8:428–433. https://doi.org/10.1016/j.culher.2007.07.004

Zuena M, Buemi LP, Stringari L, Legnaioli S, Lorenzetti G, Palleschi V, Nodari L, Tomasin P (2020) An integrated diagnostic approach to Max Ernst's painting materials in his Attirement of the Bride. J Cult Herit 43:329–337. https://doi.org/10.1016/j.culher.2019.10.010